Research article

Exploring the neuroprotection of the combination of astragaloside A, chlorogenic acid and scutellarin in treating chronic cerebral ischemia via network analysis and experimental validation

Fang Cheng [a,1], Jie Zhang [a,1], Pan Yang [a], Zufei Chen [a], Yinghao Fu [a], Jiajia Mi [a], Xingliang Xie [b,***], Sha Liu [a,**], Yanmei Sheng [a,b,*]

[a] Department of Pharmacology, School of Pharmacy, Chengdu Medical College, Chengdu, Sichuan, 610500, China
[b] The Second Class Laboratory of Traditional Chinese Medicine Pharmaceutics, National Administration of Traditional Chinese Medicine, Chengdu Medical College, Chengdu, Sichuan, 610500, China

ARTICLE INFO

ABSTRACT

Chronic cerebral ischemia (CCI) primarily causes cognitive dysfunction and other neurological impairments, yet there remains a lack of ideal therapeutic medications. The preparation combination of *Astragalus membranaceus* (Fisch.) Bunge and *Erigeron breviscapus* (Vant.) Hand.-Mazz have been utilized to ameliorate neurological dysfunction following cerebral ischemia, but material basis of its synergy remains unclear. The principal active ingredients and their optimal proportions in this combination have been identified through the oxygen and glucose deprivation (OGD) cell model, including astragaloside A, chlorogenic acid and scutellarin (ACS), and its efficacy in enhancing the survival of OGD PC12 cells surpasses that of the combination preparation. Nevertheless, mechanism of ACS against CCI remains elusive. In this study, 63 potential targets of ACS against CCI injury were obtained by network pharmacology, among which AKT1, CASP3 and TNF are the core targets. Subsequent analysis utilizing KEGG and GO suggested that PI3K/AKT pathway may play a crucial role for ACS in ameliorating CCI injury. Then, a right unilateral common carotid artery occlusion (rUCCAO) mouse model and an OGD PC12 cell model were established to replicate the pathological processes of CCI in vivo and in vitro. These models were utilized to explore the anti-CCI effects of ACS and its regulatory mechanisms, particularly focusing on PI3K/AKT pathway. The results showed that ACS facilitated the restoration of cerebral blood flow in CCI mice, enhanced the function of the central cholinergic nervous system, protected against ischemic nerve cell and mitochondrial damage, and improved cognitive function and other neurological impairments. Additionally, ACS upregulated the expression of p-PI3K, *p*-AKT, *p*-GSK3β and Bcl-2, and diminished the expression of Cyto-c, cleaved Caspase-3 and Bax significantly. However, the PI3K inhibitor (LY294002) partially reversed the downregulation of Bax, Cyto-c and cleaved Caspase-3 expression as well as the upregulation of *p*-AKT/AKT, *p*-GSK3β/GSK3β, and Bcl-2/Bax ratios. These findings suggest that ACS against neuronal damage in cerebral ischemia may be closely related to the activation of PI3K/AKT pathway. These results declared first time ACS may become an ideal candidate drug against CCI due to its

* Corresponding author. Department of Pharmacology, School of Pharmacy, Chengdu Medical College, Chengdu, Sichuan, 610500, China.
** Corresponding author.
*** Corresponding author.
   E-mail addresses: 421733038@qq.com (X. Xie), 763269850@qq.com (S. Liu), 467131233@qq.com (Y. Sheng).
  [1] These authors attribute equally to this work.
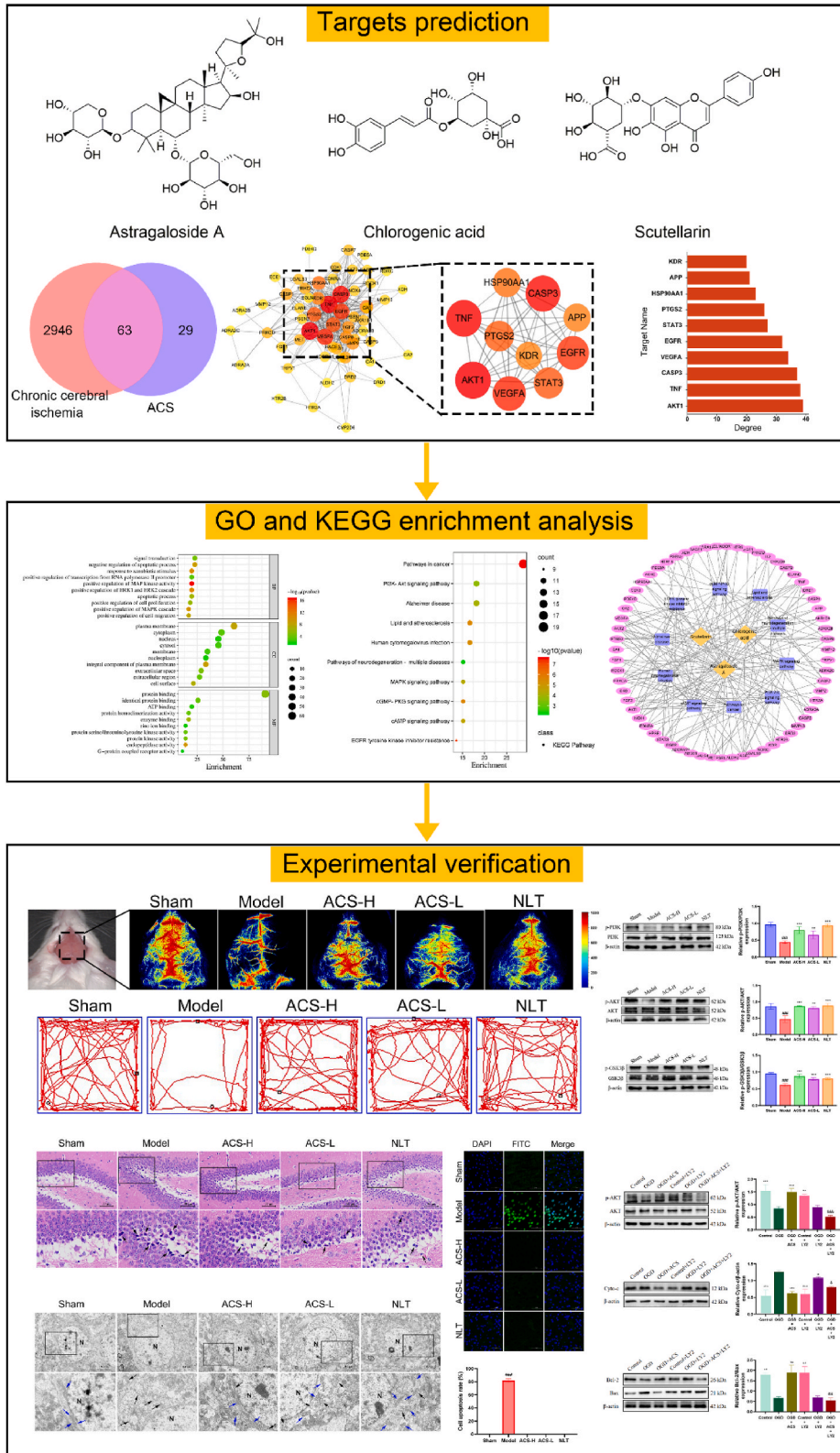
Fig. 1. The flow chart of this study.

neuroprotective effects, which are mediated by the activated PI3K/AKT pathway mitigates mitochondrial damage and prevents cell apoptosis.

1. Introduction

Chronic cerebral ischemia (CCI) refers to a condition characterized by chronic neurological dysfunction in the cerebrum resulting from reduced brain perfusion [1,2]. The aging population has been rapidly increasing in recent years, leading to a rise in the number of individuals affected by CCI. Chronic intellectual impairment syndrome, characterized primarily by cognitive dysfunction, has had a negative impact on the quality of life of patients and their families [3]. Unfortunately, there is currently no optimal pharmaceutical treatment available for CCI. Research indicates that the pathogenesis of CCI is multifaceted, involving processes such as apoptosis, oxidative stress, and immune-inflammatory damage [4–6]. Studies have shown that an ischemic-hypoxic environment can stimulate apoptosis in the hippocampus, and apoptosis, the primary form of neuronal death in ischemic cerebrovascular diseases, is closely related to the development of cognitive impairment in patients [7]. Therefore, effective prevention and management of apoptosis represent crucial strategies for reducing CCI-related injury.

Astragalus membranaceus (Fisch.) Bunge (AM) and *Erigeron breviscapus* (Vant.) Hand.-Mazz (EB) are utilized in traditional Chinese medicine (TCM) for the treatment of cerebral ischemia. AM is known for its diverse pharmacological effects, including the tonification of qi, enhancement of cerebral blood flow, and improvement of cognitive function [8,9]. Clinical research has demonstrated that AM injection exhibits antioxidative properties against ischemic injury and facilitates neurological recovery in patients [10]. On the other hand, EB is recognized for its ability to promote blood circulation [11].Studies have also shown that Erigeron injection can ameliorates cerebral ischemia/reperfusion injury in rats via modulation of mitophagy and mitochondrial apoptosis [12], improve the survival quality of patients with cerebral ischemia [13]. In TCM, Qi deficiency and blood stasis are considered the core pathogenic factors of chronic cerebral ischemia, making the invigoration of Qi and promotion of blood circulation the primary therapeutic strategies for this condition [14,15]. Therefore, the combination of AM and EB is in line with the therapeutic principle of Chinese medicine to benefit qi and invigorate blood. Clinical investigations have further revealed that the efficacy of the combination of EB injection and AM injection in the treatment of patients with cerebral ischemia is superior to that of its use alone, and improves all blood flow indexes and reduces the incidence of various complications [16].

Our previous research has demonstrated the synergistic effects of the combination of AM and EB preparation in the treatment of cerebral ischemia in rats [17,18], but the material basis of its synergy is still unclear. Furtherly, the main active ingredients and their optimal ratio have been screened through OGD cell model, including astragaloside A, chlorogenic acid and scutellarin (ACS) in our previous work [19], and its effect on promoting the survival of OGD PC12 cells is superior to that of the combination of two preparations [20]. However, the neuroprotection and potential mechanism of ACS (an optimal ingredient combination) on CCI injury are unclear.

In this present study, the mechanism of ACS against CCI injury was predicted using network pharmacology, and innovatively employed ACS for both in vivo and in vitro investigations, aiming to offer insights and scientific evidence for the development of drugs targeting the prevention and treatment of cerebral ischemic conditions. (Fig. 1).

2. Materials and methods

2.1. Animals

SPF KM mice (male, 4–5 weeks, weighing 22–26 g) were housed at the Animal Experimental Center of Chengdu Medical College (provided by Chengdu Dasuo Experimental Animal Co., Ltd., certificate No. SCXK (Sichuan) 2020-030). The experimental protocol was reviewed and approved by the Chengyi Animal Ethics Committee under batch number [2022] No. 015. The experiment was carried out after 7 days of adaptive feeding.

2.2. Drugs and reagent

Astragaloside A, sourced from Shanxi Qingya Biological (Co., Ltd., AIV-98-210902, purity≥ 98%), Chlorogenic acid from Xian Xinlu Biotechnology (Co., Ltd., EK-CHA2021091801, purity≥ 98%), and Scutellarin from Kangzhou Biotechnology (Co., Ltd., KZ-2021041201, purity≥ 98%). Naoluotong (NLT) Capsule was obtained from Guangdong Yunfang Pharmaceutical with national medicine permission number Z20063147 and batch number 20210601. Chloral hydrate was supplied by Chengdu Kelong Chemical Reagent Factory with batch number 190420. Benzylpenicillin Potassium for Injection was purchased from Jiangxi Keda Animal Pharmaceutical (Co., Ltd., 20190102).

PMSF, Phosphatase inhibitor, BCA Protein Assay Kit, RIPA lysis buffer, LY294002 (inhibitor of phosphatidylinositol 3-kinase, S1737-25 mg) and cleaved Caspase 3 rabbit monoclonal antibody (AF1150, 1: 1000) were provided by Beyotime Biotechnology (Shanghai, China). SOD, MDA, GSH-Px, CAT, ChE, CHAc assay (ELISA) kits were supplied by Enzyme-Linked Biotechnology (Shanghai). PI3K (20584-1-AP, 1: 500), AKT (60203-2-Ig, 1: 5000), *p*-AKT (66444-1-Ig, 1: 5000), GSK3β (22104-1-AP, 1: 4000), Bax (60267-1-Ig, 1: 10000), Bcl-2 (26593-1-AP, 1: 2000) and Cyto-c (10993-1-AP, 1: 4000) were supplied by Proteintech (Wuhan, China); p-PI3K (AF3242, diluted 1: 500) and *p*-GSK3β (AF2016, diluted 1: 1000) were provided by Affinity Biosciences (Cincinnati, OH, USA).

2.3. Prediction of component targets and Collection of CCI-related genes

Each component's SMILES were gained from the common database PubChem (https://pubchem.ncbi.nlm.nih.gov/) [21]. Swiss Target Prediction (http://www.swisstargetprediction.ch/) [22] was used to obtain the relevant targets for each component. Subsequently, the obtained data were aggregated to establish a combined preparation active ingredients-targets data set. Using "chronic cerebral ischemia" as the keyword, we searched the databases OMIM (https://omim.org/), GeneCards (https://www.genecards.org/) [23] and DisGeNET (https://www.disgenet.org/home/) [24] to obtain CCI related targets, and combined the three search results to get CCI targets [25].

2.4. Network establishment and analysis methods

The VENNY2.1 online software (https://bioinfogp.cnb.csic.es/tools/venny/) [26] was utilized to plot the Venn diagram and take components intersection targets acting on CCI. The STRING 11.0 database (https://stringdb.org) was used to construct a protein-protein interaction (PPI) network after setting the minimum interaction threshold (>0.4) [27,28]. For further analysis, the PPI data was imported into Cytoscape 3.9.1 software (https://cytoscape.org/). Input the intersection targets into the DAVID database (https://david.ncifcrf.gov/), limit the species to "Homo sapiens", set $P < 0.05$, and perform Gene Ontology (GO) and KEGG pathway enrichment analyses [29]. Then the major pathways, components and 63 intersection targets were used to construct a "component-target-pathway" map.

2.5. Establishment of rUCCAO model

Mice were fed with fasting without water for 12 h, 10% chloral hydrate (0.1 mL/20 g) was anesthetized by intraperitoneal injection. Immobilize in a supine position and keep breathing smoothly, and then the mouse model of CCI was established by rUCCAO method [30,31]. In sham group only separated the right common carotid artery. To prevent infection, each group of mice received an intramuscular injection of 200,000 units/kg Benzylpenicillin Potassium for three days.

2.6. Grouping and drug administration

60 KM mice were divided into 5 groups: sham, model, ACS-L (astragaloside A: chlorogenic acid: scutellarin = 14: 42: 28 mg kg^{-1}) and ACS-H (astragaloside A: chlorogenic acid: scutellarin = 28: 84: 56 mg kg^{-1}) and positive group (NLT, 195 mg kg^{-1}). Combined with the optimal ratio of ACS (astragaloside A, chlorogenic acid and scutellarin = 1: 3: 2) screened by our previous work [19], and the maximum dosage of astragaloside A in cerebral ischemia rats is 20 mg kg^{-1} [32]. According to the dose conversion coefficient (1.4 times) between rat and mouse, the dosage of astragaloside A in mice was calculated to be 28 mg kg^{-1}, so chlorogenic acid and scutellarin was 84 mg kg^{-1} and 56 mg kg^{-1} respectively in the ACS-H group of CCI mice, and the dosage of ACS-L group can be obtained by corresponding dilution of the dose of ACS-H group. The dose of NLT capsule was calculated according to the conversion coefficient body surface area between human and mouse when the clinical human dose is 1.5 g per day. The mice in ACS and NLT groups were orally administered drugs once a day for 30 days after surgery, while the mice in sham and model groups administered an equal volume of normal saline.

2.7. Open field trial

The open-field activity testing system (OFT-100, Taimeng) for mice and rats was used to assess the spontaneous and exploratory behaviour of each mouse [33]. The open-field box was made of smooth blackboards (40 cm in length, width and height). A digital camera was placed 1 m above the box to record mice' movement across the entire field of view. The mouse was placed in the center of a square area, and the number of times they stood up in 5 min, as well as the distance they moved in the center, was recorded and tested for 3 days. To avoid the odour, the entire field cleaned with 75% ethanol at the end of each test.

2.8. Laser speckle imaging system detection of cerebral blood flow (CBF)

We utilized the system of laser speckle imaging (RFLSI III, RWD) to monitor CBF after surgery immediately (namely administration for 0 days) and administration for 30 days separately, and the change in CBF was calculated. Right CBF decline rate = (right CBF - left CBF)/left CBF; recovery rate of right CBF (%) = (right CBF decline rate after administration 30 days-right CBF decline rate after administration 0 days)/right CBF decline rate administration 0 days × 100%; recovery rate of global CBF (%) = (global blood flow after administration 30 days - global blood flow after administration 0 days)/global blood flow administration 0 days × 100%).

2.9. HE staining

To estimate pathological changes, HE staining was conducted as the previous method (Yang et al., 2022). Mouse brain tissues were soaked in 4% paraformaldehyde, then routinely dehydrated, transparent, etc. Finally, the cell structure of the cerebral sample was watched under a microscope.

2.10. TUNEL staining

After fixation, embedding and sectioning, cerebral tissues were subjected to in situ apoptosis assay according to the Kit' instructions. Five non-overlapping fields were picked under a microscope of 200 × randomly. The normal nucleus turned blue and the apoptosis-positive cells green. Apoptosis rate (%) = apoptosis-positive cells/(apoptosis-positive cells + number of normal cells) × 100%.

2.11. TEM assay

The hippocampal tissue was treated with an electron microscopy fixator and 1% osmic acid × phosphate buffer (PB, 0.1 M), respectively 2 h at room temperature (RT). Rinsed with 0.1 M PB (pH = 7.4) 3 times, 15 min/time. Dehydrated with gradient ethanol, infiltrated and embedded in acetone, made into ultrathin sections (60–80 mm), double-dyed with uranium and lead (15 min respectively), sections were dried at RT overnight, and the ultrastructure of mitochondria in the hippocampus was observed under the TEM.

2.12. Determination of SOD, GSH-Px, CAT and MDA content

Leave the test tubes containing blood stand in a 37 °C water bath for 30 min, then centrifuge at 3000 r/min (15 min). The levels of SOD, GSH-Px, CAT and MDA were measured according to the kit' directions.

2.13. Determination of ChE and CHAc in the hippocampus

Hippocampal tissue was homogenized in a tube containing pre-cooled normal saline (tissue weight (g): volume (mL) = 1: 9), and centrifuged (3000 r/min, 10 min). Subsequently, the supernatant was collected for testing as directed.

2.14. Cell culture

PC12 cells were obtained from the Chinese Academy of Sciences, cultured in DMEM supplemented with 10% FBS, 100 U/mL Penicillin, and 100 μg/mL Streptomycin. The cells were cultured at 37 °C in an incubator supplemented with 5% CO_2 and sub-cultured every 2 or 3 days. Cells at passages 4–8 were used for all experiments.

2.15. Oxygen and glucose deprivation mode and grouping

The logarithmic growth phase PC12 cells were taken and the cell number was adjusted to 1×10^6 cells/well and inoculated in 6-well plates for 24 h. The cells were divided into following groups: Control, OGD, OGD + ACS, Control + LY294002, OGD + LY294002, OGD + ACS + LY294002. PC12 cells were pretreated with ACS and LY294002 at 24 h and 1 h before OGD, respectively. Subsequently, the cell culture medium was changed to sugar-free medium for the model and each administration group and incubated in a constant and closed hypoxic chamber (95% N2 and 5% CO2) at 37 °C for 2 h. The effective ACS concentration acting on the cells was astragaloside A: chlorogenic acid:scutellarin (ACS) = 10: 75: 45 μM [34], and the effective concentration of LY294002 was 10 μM.

2.16. Western blot analysis

After treatment with OGD or rUCCAO, PC12 cells and mouse hippocampal tissue were lysed on ice with RIPA lysis solution. The protein concentration was determined using the BCA method. Then proteins were separated by 12% SDS-PAGE concentrated glue and transferred onto PVDF membranes. The membranes blocking with 5% skimmed milk powder (1.5 h), washed with TBST (3 times), incubated (24 h, 4 °C) and then primary antibodies (PI3K, p-PI3K, AKT, *p*-AKT, GSK3β, *p*-GSK3β, Cyto-c, cleaved-Caspase-3, Bax, Bcl-2; dilution ratio shown in the section "Drugs and reagent") were added. Next, the membranes were rinsed with TBST (3 times), followed by incubating in secondary antibody at 37 °C (1.5 h, diluted 1: 5000), and washed with TBST as mentioned above; Combined with ECL chemiluminescence imaging, a gel imaging system was used to obtain images. Finally, the gray values of the proteins were quantified using Image-J software 1.8.0 (NIH) with β-actin or α-tubulin as the comparative internal control.

2.17. Statistical analysis

All data were analyzed using SPSS 26.0 statistical software (SPSS Inc., Chicago, IL, USA). One-way analysis of variance was used for measurement data conforming to normal distribution and homogeneity of variance, and measurement data with skewed distribution were compared between groups by the Kruskal-Wallis method. Numerical data were expressed as "mean ± standard deviation" ($\bar{x} \pm$ s). $P < 0.05$ was considered to show a statistically significant difference.

3. Results

3.1. Potential targets of components and CCI genes

Ninety-two component targets were obtained from PubChem and Swiss database (Table 1). And among the total of 3009 CCI-related targets obtained from OMIM, GeneCards and DisGeNET databases, 63 were found to be associated with ACS (Fig. 2A).

3.2. PPI network analysis

The PPI network was constructed via STRING 11.0 with a threshold (>0.4) and visualized with Cytoscape software (Fig. 2B). This PPI network included 59 nodes and 335 edges. A circular node represented a target, and the bigger the more important. Then selecting the top 10 targets for ranking and visualization analysis. Those were AKT1, TNF, CASP3, VEGFA, EGFR, STAT3, PTGS2, HSP90AA1, APP, KDR (Fig. 2C).

3.3. Enrichment analysis

GO analysis and KEGG analysis were performed on 63 common target genes using the DAVID database. The screening bases on $P <$ 0.05, and after sorting according to count, representative pathways were selected as important pathways and visualized for analysis. The results shown in Fig. 3A. ACS was involved in regulating BP of CCI, including signal transduction, negative regulation of the apoptotic process, positive regulation of transcription from RNA polymerase II promoter, response to xenobiotic stimulus, etc. The cell component was mainly enriched in the plasma membrane, cytoplasm, cytosol, etc. The molecular function was closely associated with protein binding, identical protein binding, ATP binding, etc. The mechanism of action of ACS on CCI mainly involved signal pathways such as Pathway in cancer, Alzheimer disease, PI3K-AKT, and MAPK signal pathway, etc (Fig. 3B). The enriched targets and other information for each pathway are shown in Table 2. Finally, imported 63 targets of ACS related to CCI and the main signal pathways involved in Cytoscape software for visualization, and structured a "component-target-pathway" map (Fig. 4).

3.4. Open field trial

In this study, the motor function and cognitive impairment in CCI mice were assessed using the open field trial. As displayed in Fig. 5A–C, there was a significantly reduction in standing times, and the central movement distance in the model group ($P < 0.001$). After ACS treatment, the standing times, the central area exploration behaviour and the distance of central movement were significantly exceeded the CCI model group ($P < 0.001$). These suggested that ACS effectively upgraded autonomic activity and cognitive dysfunction of CCI mice.

3.5. Effects of ACS on CBF in mice with CCI

Fig. 6B showed that the CBF difference between the left and right sides of mice with CCI on day 0 of administration was significantly increased ($P < 0.001$), indicating that the CCI model succeeded. Fig. 6A, **C, D** and **E** showed that after 30 days of ACS treatment, CBF in ACS-H and ACS-L groups were significantly recovered ($P < 0.001$).

3.6. Effects of ACS on the levels of SOD, GSH-Px, CAT and MDA

As demonstrated in Fig. 7A–D, the CCI model group had a decrease in the level of SOD, GSH-Px, and CAT, while an increase in MDA content ($P < 0.001$). However, ACS enhanced the level of SOD, GSH-Px and CAT, and diminished MDA content ($P < 0.001$).

Table 1
The SMILES and related targets of component.

Component	SMILES	Targets
astragaloside A	CC1(C(CCC23C1C(CC4C2(C3)CCC5(C4 (CC(C5C6(CCC(O6)C(C)(C)O)C)C)C)OC7C(C(C(C(O7)CO)O)O)O)OC8C(C(C(CO8)O)O)O)C	PSEN2, HSP90AA1, VEGFA, FGF1, FGF2, HPSE, LGALS4, LGALS3, LGALS8, HTR2B, ADRA2A, ADRA2C, ADRA2B, DRD1, ADRA1D, CYP2D6, HTR6, ADRA1A, HTR1B, PTPRA, PTPN2, CDK1, AKT2, RPS6KA1, ROCK1, AKT1, STAT3, MET, PSENEN, NCSTN, APH1A, PSEN1, APH1B, RORC, TOP1, DRD2, HTR2A, DRD3, TRPV1, AKR1B1, TNF, IL2, ADORA1, XDH, RPS6KA3, NMUR2, ACHE, CA2, NQO2, PTGS2, PRKCA, NOX4, CA12, ADORA2B, ALDH2
chlorogenic acid	C1C(C(C(C(CC1(C (=O)O)O)OC(=O)C=CC2=CC(=C(C=C2)O)O)O)O	AKR1B1, AKR1B10, MMP13, MMP2, MMP12, APP, ELANE, SLC37A4, PYGL, PRKCD, PRKCA, BACE1, PDE5A, PDE4D, PDE9A, PDE1B, CA2, CA1, CA12, CA9, CA5B, EDNRA, ABCB1, NEU4, CASP3, KDR, ENGASE, NEU3, NEU2, OGA, TREH, CASP6, CASP7, CASP8, CASP1, CASP2, ECE1, EGLN1, ADAMTS5, FTO
scutellarin	C1=CC(=CC=C1C2=CC(=O)C3=C(C(=C(C=C3O2)OC4C(C(C(C(O4)C (=O)O)O)O)O)O)O)O	AKR1B1, ADORA1, XDH, TNF, IL2, PTGS2, RPS6KA3, ACHE, NQO2, NOX4, ADRA2C, NMUR2, ADRA2A, EGFR, CA2, CA12
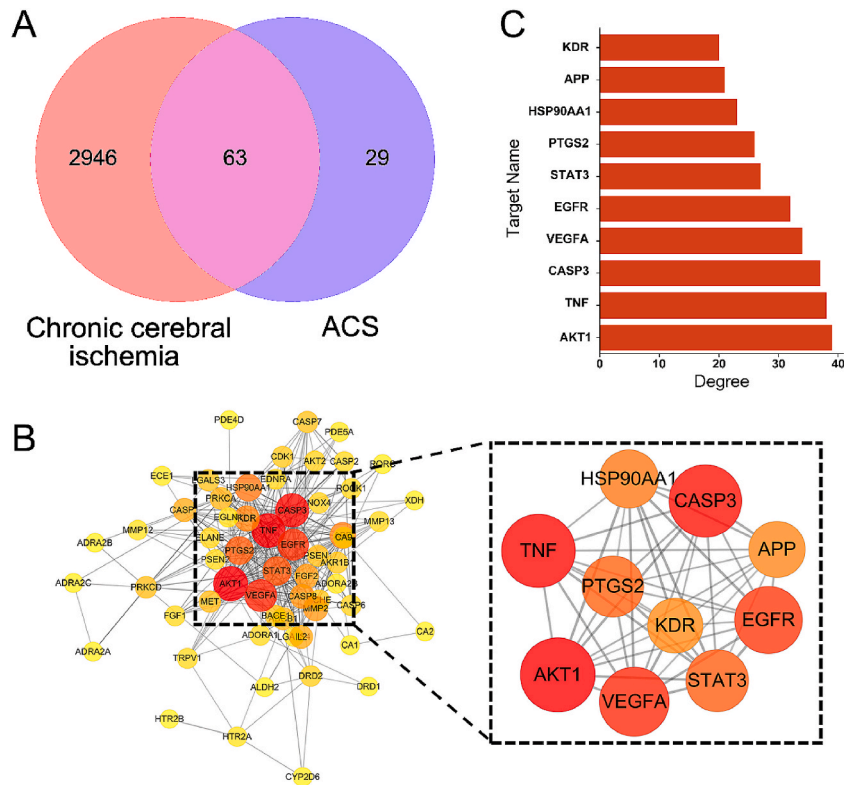
Fig. 2. Venn diagram and PPI network (**A**) Venn diagram of component target-disease. (**B**) PPI network of 63 disease-drug co-targets and top 10 core targets in terms of degree. The node increases with the degree value. (**C**) Rank the top 10 core targets by degree.
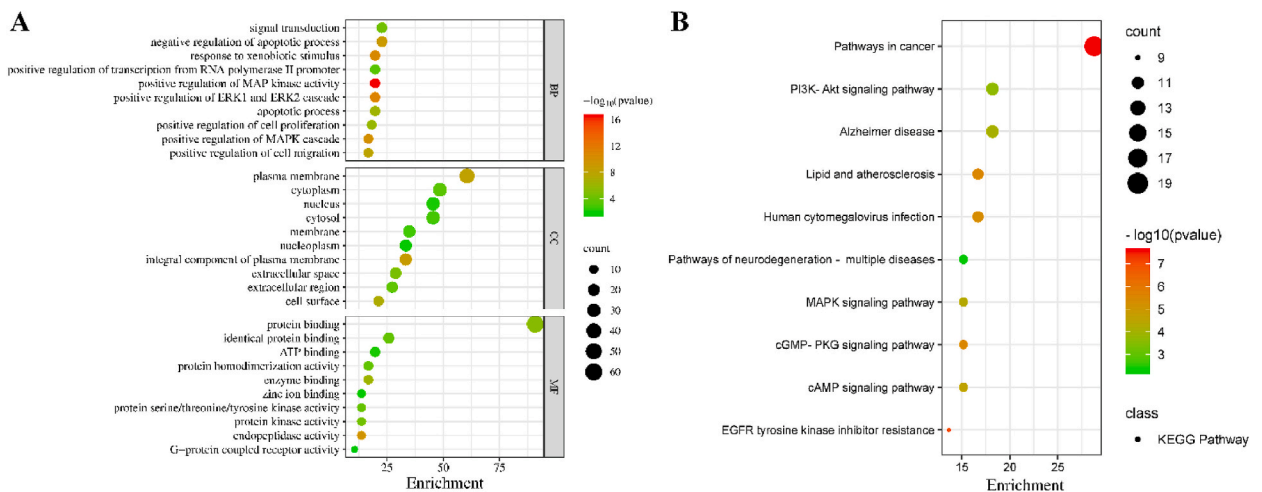
Fig. 3. GO enrichment, KEGG analysis (**A**) GO analysis. (**B**) The chart of KEGG analysis, the circle becomes larger with the increase in the target count.

3.7. Effects of ACS on the levels of ChE and CHAc in the hippocampus

ChE and CHAc jointly maintained the dynamic balance of Ach in the central cholinergic system. They enhanced the function of the central cholinergic system, which could effectively alleviate the cognitive dysfunction caused by CCI injury. According to Fig. 7E and F, the ChE content of the model group was significantly enhanced, and the CHAc level reduced ($P < 0.001$). However, ACS greatly enhanced the CHAc level ($P < 0.001$) and lessen the ChE content ($P < 0.01$).

Table 2
The KEGG top 10 pathway related information.

Term	Count	P Value	Genes
Pathways in cancer	19	2.15E-08	EGLN1, HSP90AA1, ROCK1, MMP2, STAT3, PRKCA, FGF1, PTGS2, FGF2, EGFR, IL2, VEGFA, CASP7, EDNRA, CASP8, CASP3, AKT2, AKT1, MET
Alzheimer disease	12	8.83E-05	BACE1, APP, CASP7, CASP8, AKT2, CASP3, PSEN2, NOX4, AKT1, PSEN1, PTGS2, TNF
PI3K-Akt signaling pathway	12	2.16E-04	HSP90AA1, AKT2, KDR, AKT1, PRKCA, FGF1, FGF2, MET, EGFR, IL2, VEGFA, CASP3
Lipid and atherosclerosis	11	2.97E-06	CASP7, HSP90AA1, CASP8, CASP6, AKT2, CASP3, STAT3, CASP1, AKT1, PRKCA, TNF
Human cytomegalovirus infection	11	4.47E-06	CASP8, ROCK1, AKT2, CASP3, STAT3, AKT1, PRKCA, PTGS2, TNF, EGFR, VEGFA
MAPK signaling pathway	10	4.61E-05	AKT2, CASP3, KDR, AKT1, PRKCA, FGF1, TNF, FGF2, MET, EGFR
cGMP-PKG signaling pathway	10	2.93E-06	EDNRA, ROCK1, AKT2, ADORA1, AKT1, PDE5A, ADRA2C, ADRA1A, ADRA2B, ADRA2A
cAMP signaling pathway	10	2.84E-05	HTR6, EDNRA, ROCK1, AKT2, PDE4D, ADORA1, HTR1B, AKT1, DRD1, DRD2
Pathways of neurodegeneration-multiple diseases	10	7.24E-03	APP, CASP7, CASP8, CASP3, PSEN2, NOX4, PRKCA, PSEN1, PTGS2, TNF
EGFR tyrosine kinase inhibitor resistance	9	8.80E-08	AKT2, STAT3, KDR, AKT1, PRKCA, FGF2, MET, EGFR, VEGFA

Fig. 4. Diagram of "component-target-pathway". Light yellow represents ACS; Blue represents the major signaling pathways; Purple represents the target.

3.8. HE staining

As demonstrated in Fig. 8A, hippocampal neurons in the sham group had complete structure, and their cell nucleoli were clear with uniform staining. However, a few nerve cells in the model group had abnormal morphology, deep-stained solid contraction, and irregular arrangement. Interestingly, ACS effectively ameliorated the damage to hippocampal neurons.

Fig. 5. The times of standing, movement distance in the central court, and movement trajectory in open field trial. (**A**) standing times. (**B**) movement trajectory. (**C**) movement distance in the central court. Data were presented as mean ± SD. (n = 10). $^{###}p < 0.001$ *vs* sham group; $^{***}p < 0.001$ *vs* model group.
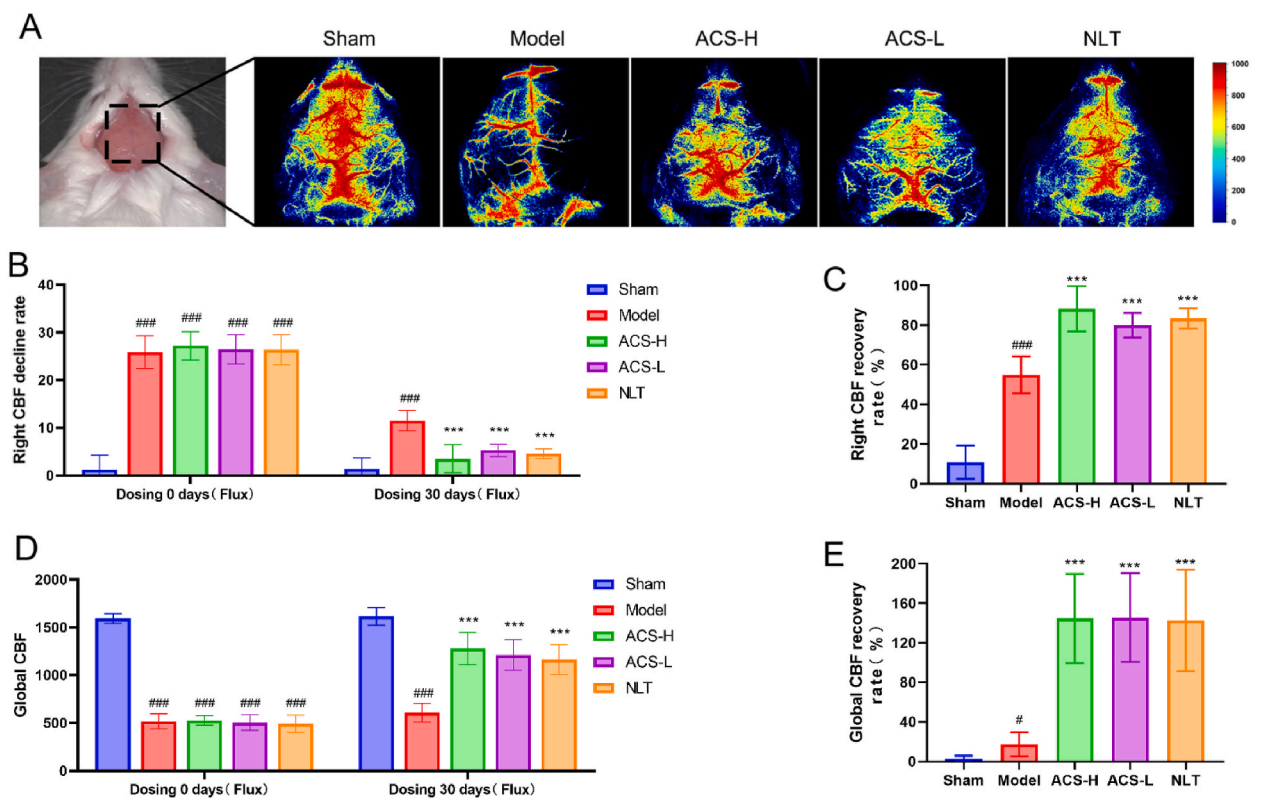
Fig. 6. CBF detected by Laser speckle imaging system. (**A**) Images of laser speckle blood flow detection. (**B, C**) The CBF difference between left and right and recovery rate of right CBF. (**D, E**) Global CBF and its recovery rate. Data were expressed as mean ± SD (n = 10). $^{###}p < 0.001$ *vs* sham group; $^{***}p < 0.001$ *vs* model group.
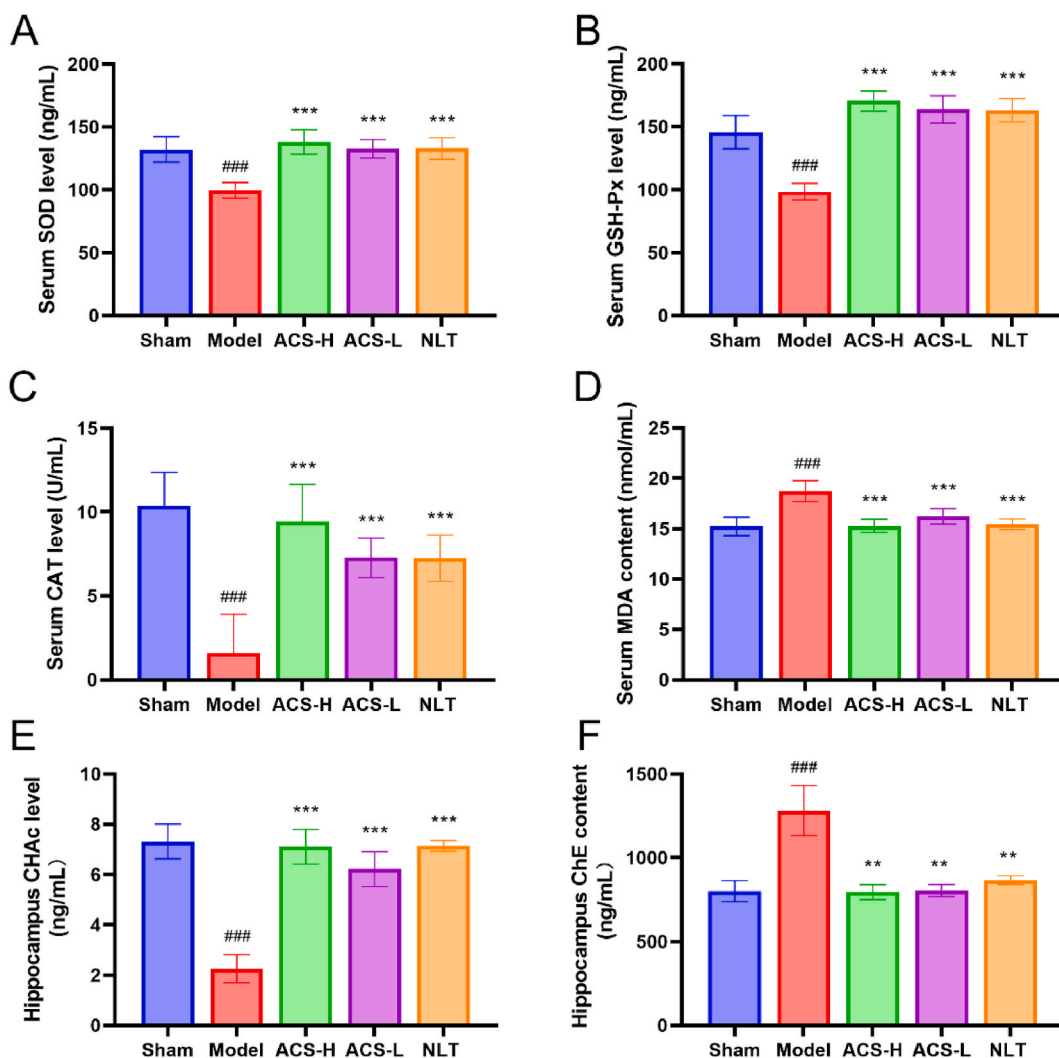
Fig. 7. Effects of ACS on oxidative injury in CCI mice. (**A**) Serum SOD level. (**B**) Serum GSH-Px level. (**C**) Serum CAT level. (**D**) Serum MDA content. (**E**) Hippocampal CHAc level. (**F**) Hippocampal ChE content. Data were presented as mean ± SD (n = 7). $^{##}p < 0.01$ and $^{###}p < 0.001$ *vs* sham group; $^{**}p < 0.01$ and $^{***}p < 0.001$ *vs* model group.

3.9. Effects of ACS on neuronal apoptosis in cerebral tissue

The apoptosis in cerebral tissue was measured by TUNEL staining (Fig. 8C and D). The CCI model group had more TUNEL positive cells and higher apoptotic rate, which were considerably lessened with ACS treatment ($P < 0.001$).

3.10. Effects of ACS on mitochondrial structure in hippocampus by TEM

The mitochondria in the hippocampal nerve cells had regular shapes and apparent outlines in sham group (Fig. 8B). Whereas, the mitochondria severely swollen was observed in the CCI mice, with partial membrane bulging, blurred and damaged structures, massive dissolution of the matrix, the disappearance of cristae, and vacuolization. What's more, ACS significantly could improve mitochondrial damage, and increase the number of cristae.

3.11. The effects of ACS on PI3K/AKT pathway related proteins

The expression of proteins relevant to PI3K/AKT pathway was detected by Western blot (WB). The CCI model group had a decline in the ratios of p-PI3K/PI3K (Fig. 9A and B), *p*-AKT/AKT (Fig. 9C, D), and *p*-GSK3β/GSK3β (Fig. 9E and F) which were remarkably up-regulated by ACS administration ($P < 0.05$). These results indicated that ACS resisting CCI injury by modulating PI3K/AKT pathway.

The expression of proteins related to the apoptosis was quantified by WB. The results revealed that the enhanced expressions of
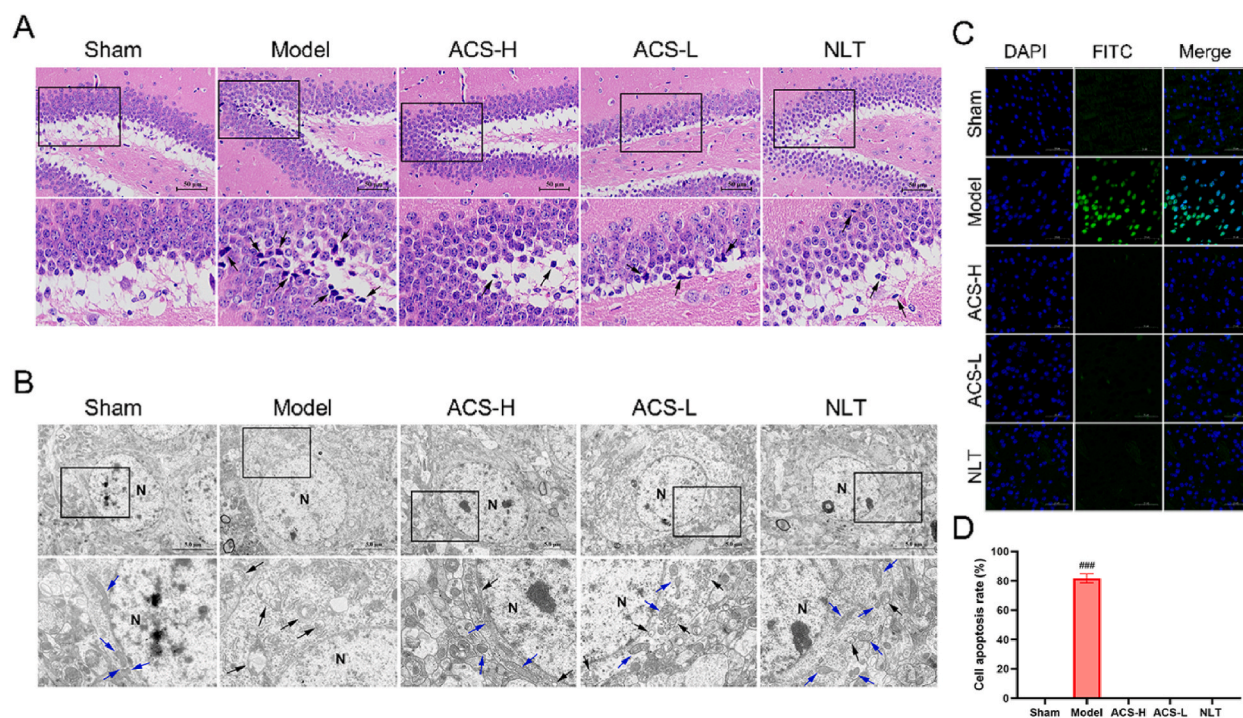
Fig. 8. The effects of ACS on CCI-induced pathological injury, neuronal apoptosis and mitochondria damage in CCI mice. (**A**) Representative images of HE staining (400 ×). Deep-stained solid contraction neurons (black arrows). (**B**) Normal mitochondria (blue arrows) and injured mitochondria (black arrows). (**C**) Images of TUNEL staining (200 ×). Green fluorescence represents TUNEL positive cells. (**D**) The cell apoptosis rate. Data were represented as mean $\pm$ SD (n = 3). $^{\#\#\#}p < 0.001$ *vs* sham group.

Cyto-c (Fig. 10A and B), cleaved Caspase-3 (**Fig, 10C, D**) and Bax (Fig. 10E–G) in ischemic hippocampus were reversed by ACS administration. While ACS markedly upregulated the levels of Bcl-2 and Bcl-2/Bax ratio ($P < 0.05$, Fig. 10F–H). These findings confirmed that ACS exerted a chief apoptotic repression on CCI damage.

To further investigate whether ACS alleviates apoptotic neuronal damage in brain ischemia through activation of PI3K/AKT pathway, the PI3K inhibitor LY2940002 (10 μM) was selected for validation in *vitro* study. The results showed that LY294002 reversed the downregulation of Cyto-c (Fig. 11E and F), cleaved Caspase-3 (Fig. 12A and B) and Bax (Fig. 12C–F) expression and the upregulation of p-AKT/AKT (Fig. 11A, B), p-GSK3β/GSK3β (Fig. 11C and D) and Bcl-2/Bax expression ratios (Fig. 12 D, E). These results suggest that ACS against apoptotic neuronal damage in cerebral ischemia may be closely related to the activation of PI3K/AKT pathway.

4. Discussion

With the acceleration of China's aging population and changes in lifestyle, the incidence of cerebrovascular diseases is on the rise [35]. Studies have shown that a common pathological factor in most cerebrovascular diseases is CCI, with long-term cerebral hypoperfusion being a primary cause of neurological damage and cognitive impairment in patients [3]. Therefore, there is significant social value and theoretical importance in investigating the pathogenesis of CCI and identifying effective prevention methods.

The preparation combination of AM and EB has been widely utilized in cerebrovascular disease research [17,18,36]. Traditional Chinese Medicine (TCM) comprises a complex array of active ingredients with multi-target pharmacological actions. If we could screen more formulae with precise active ingredients and significant efficacy from TCM, it would be helpful to promote the development and application of ingredient combinations. This exploration may offer fresh perspectives for the creation of innovative Chinese medicines for related diseases.

With the development of TCM modernization, network pharmacology reveals the influence of drugs on disease networks more systematically and holistically. This research strategy aligns with the synergistic nature of TCM's multi-component, multi-target characteristics, as well as the holistic treatment philosophy of TCM [37,38]. In this study, the network pharmacology was used to screen 63 potential targets of ACS against CCI injury. PPI network and topological analysis showed that AKT1, CASP3 and TNF were the core targets. KEGG analysis showed that the regulation of CCI by ACS involves multiple signaling pathways, and in addition to the cancer pathway, the PI3K/AKT signaling pathway may be the most critical mechanism, which either regulates AKT1, CASP3, HSP90AA1, VEGFA and other key targets to play an anti-ischemic neurological injury role in the brain.

To validate the findings of network pharmacology, a CCI model was induced using the rUCCAO method to investigate the
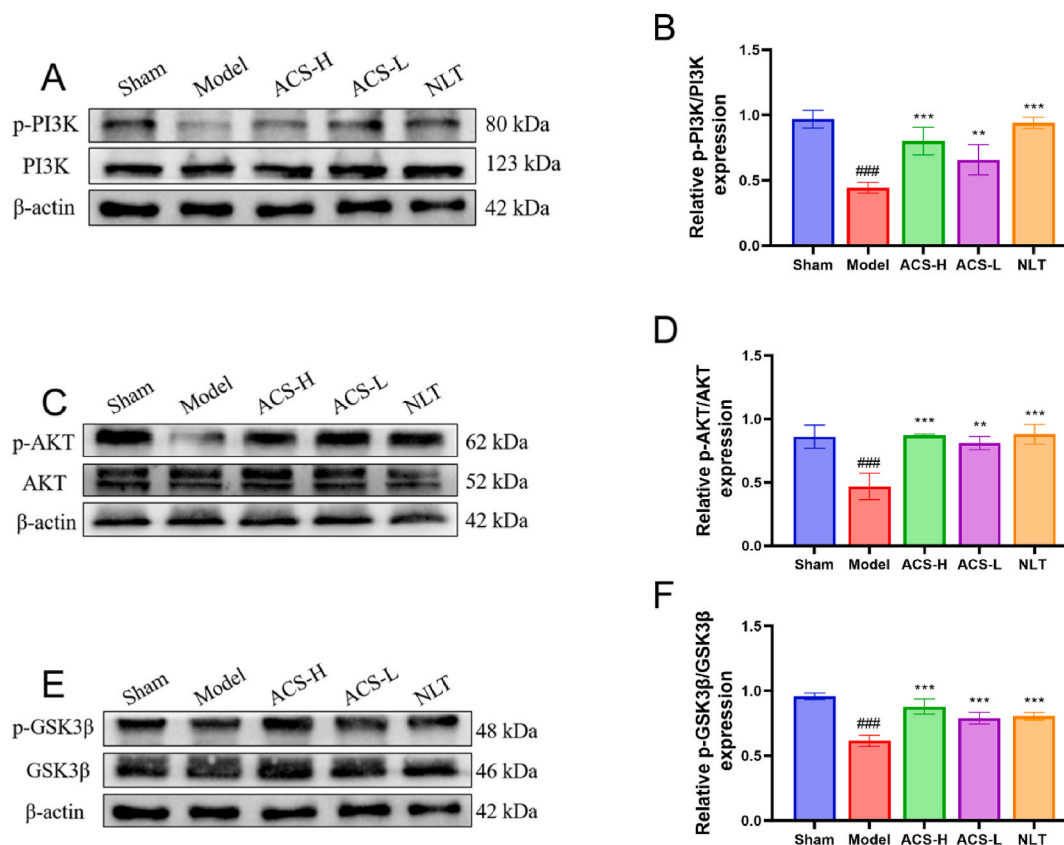
Fig. 9. ACS activated PI3K/AKT pathway. WB analysis of PI3K, p-PI3K (**A, B**), AKT, *p*-AKT (**C, D**), GSK3β, *p*-GSK3β (**E, F**). Full-length gels before cropping are noted in fig. S1. Data were presented as mean ± SD. (n = 3). $^{\#}p < 0.05$, $^{\#\#}p < 0.01$ and $^{\#\#\#}p < 0.001$ *vs* sham group; $^{*}p < 0.05$, $^{**}p < 0.01$ and $^{***}p < 0.001$ *vs* model group.

neuroprotective effects and mechanisms of ACS. Various animal models can be utilized for CCI research, including rUCCAO and 2-vessel occlusion (2-VO) models [39]. The 2-VO obstruction model can be used to simulate learning and memory, cerebral blood flow, neuropathological changes and other characteristics caused by chronic cerebral hypoperfusion and white matter injury [40]. However, ligation of bilateral common carotid arteries at the same time can easily cause acute brain injury, severe heart burden and high mortality in animals due to rapid decrease in blood flow and increase in blood pressure [41]. The rUCCAO method is commonly employed in experimental CCI studies due to its lower mortality rate, which ensures a sustained mild reduction in cerebral blood flow and the development of cognitive dysfunction associated with cerebral ischemia [42,43].

It has been observed that the morphological basis of cognitive dysfunction induced by CCI is linked to cholinergic neuron dysfunction. The dysfunction of the cholinergic system is primarily characterized by an increase in ChE content, a decrease in CHAc activity, and Ach levels [44,45]. In this study, the CBF and the CHAc activity were significantly reduced, the ChE content was increased, and spatial exploration ability and autonomous activity ability were weakened of the CCI mice, which were dramatically reversed by ACS administration. These suggested that ACS could effectively promote the recovery of CBF in CCI mice, and then improve the cognitive dysfunction by enhancing the function of the central cholinergic system, such as learning function and exploration ability.

Oxidative stress plays an important role in cerebral ischemic injury and can affect all stages of CCI in many ways [46]. In addition to providing sufficient energy to maintain nerve cell excitability and cell survival, mitochondria were also the main base for reactive oxygen species (ROS) generation [47,48]. Long-term cerebral blood flow hypoperfusion caused an imbalance between the oxidative and antioxidant systems. A large amount of ROS produced in the body reduced the content of antioxidant enzymes, weakened the scavenging ability of ROS, and aggravated oxidative stress. Then again, ROS acted on the lipid, protein and DNA of mitochondria, causing oxidative damage, affecting electron transport function, and damaging mitochondrial structure and function. Mitochondrial damage led to increase the release of ROS, which in turn induced cell death [49,50]. In this study, TEM was utilized to examine hippocampal neuron mitochondria. We observed severe mitochondrial edema, cristae disruption, and vacuolization in CCI mice, while treatment with ACS partially alleviated mitochondrial structural damage. Additionally, the MDA level, a marker of oxidative stress damage, was found to decrease with ACS treatment, indicating a reduction in oxidative stress-induced damage [51]. The results showed that MDA content was significantly increased, and the expression of antioxidant enzymes and proteins, such as SOD, GSH-Px, CAT weakened considerably in CCI mice. Notably, ACS treatment could reverse the decreased enzymes of antioxidant damage above,
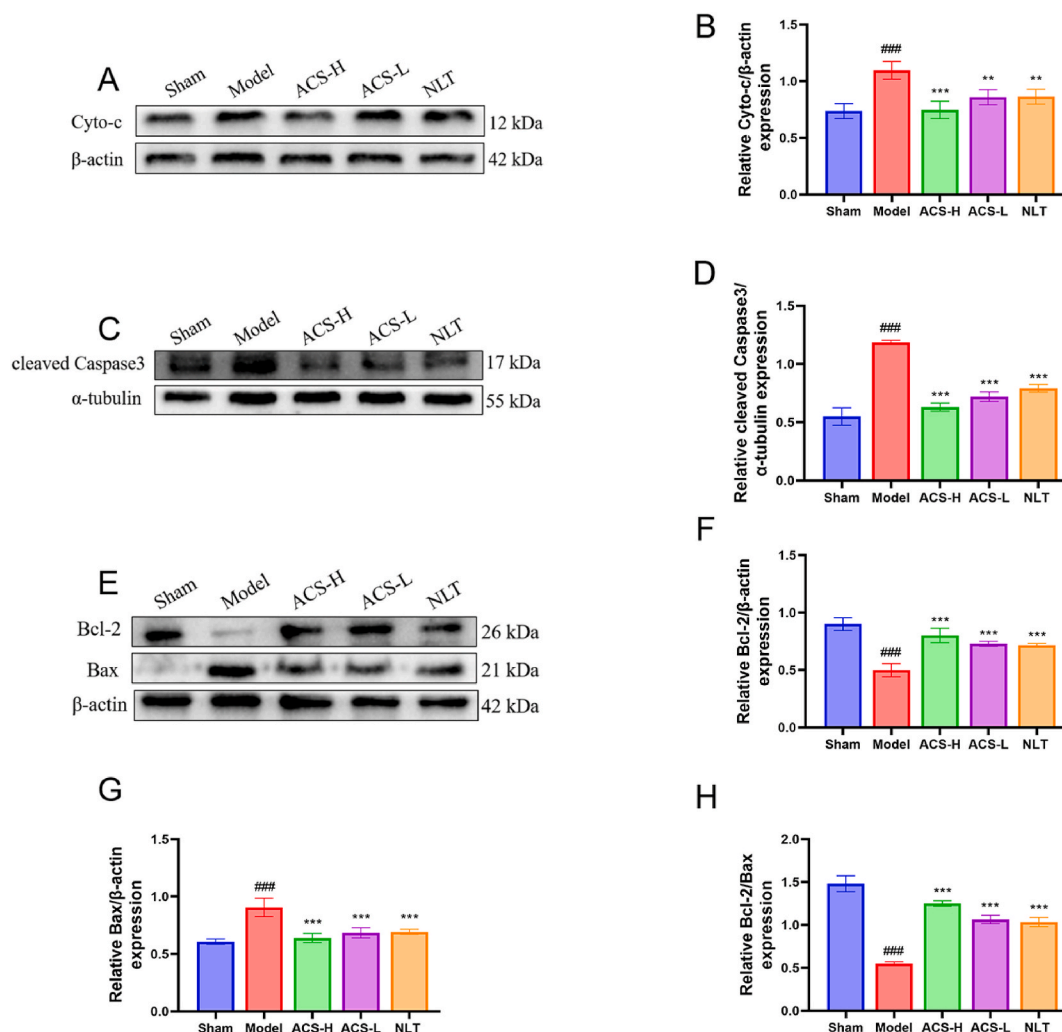
Fig. 10. ACS down-regulated Cyto-c, Bax, cleaved-Caspase3 expression in hippocampus. WB analysis of Cyto-c (**A, B**), cleaved-Caspase3 (**C, D**), Bcl-2, Bax, Bcl-2/Bax (**E-H**). Full-length gels before cropping are noted in fig. S2. Data were presented as mean $\pm$ SD (n = 3). $^{\#}p < 0.05$, $^{\#\#}p < 0.01$ and $^{\#\#\#}p < 0.001$ vs sham group; $^{*}p < 0.05$, $^{**}p < 0.01$ and $^{***}p < 0.001$ vs model group.

along with an increase in MDA content. These findings validated that ACS could effectively improve mitochondrial dysfunction, reduce the generation of reactive oxygen species and oxidative product, and improve the level of antioxidant enzymes.

Long-term cerebral hypoperfusion has the potential to harm the cerebral cortex and hippocampus, neurons in the hippocampal CA1 area and frontal cortex of rats with CCI-induced cognitive impairment were disorganized and underwent massive apoptosis [52]. HE staining revealed alterations in the structure of nerve cells in the hippocampal region of CCI model mice, including nuclear disappearance, solidification into shuttle and triangular shapes, and sparse and disordered arrangement of nerve cells compared to the sham group. Treatment with ACS was able to mitigate the damage to nerve cells in the hippocampus. In order to further explore the degree of nerve cell injury and the protective effect of ACS on brain tissue, TUNEL staining revealed that ACS could significantly reduce the apoptosis of nerve cells in the cortex of the model mice, implying a neuroprotective effect. The PI3K/AKT pathway plays a crucial role in cell survival and apoptosis inhibition [53]. During cerebral ischemia or hypoxia, PI3K is activated, leading to the activation of AKT. Activated AKT can regulate cell growth, differentiation, and migration by activating GSK3β through direct or indirect pathways. Furthermore, AKT can indirectly inhibit the release of Cytochrome c by modulating the expression of Bcl-2 family proteins, ultimately reducing the expression of the apoptosis executioner protein Caspase-3 [12,54,55]. Relevant studies have confirmed that the activation of PI3K/AKT pathway can diminish the expression of the pro-apoptotic protein Bax, Cyto-c and promote the expression of the anti-apoptotic protein Bcl-2, resulting in an anti-apoptotic effect [56]. Results from in vivo studies indicated that the ratios of p-PI3K/PI3K, p-AKT/AKT, p-GSK3β/GSK3β and Bcl-2/Bax were significantly decreased in model group, accompanied by elevated levels of Cyto-c, Bax, and cleaved Caspase-3. However, treatment with ACS reversed the expression levels of these proteins. To investigate the causal relationship between ACS and the PI3K/AKT pathway, an in vitro study was conducted using the PI3K inhibitor LY294002. The results confirmed that LY294002 reversed the positive regulatory effect of ACS on this pathway, indicating that ACS
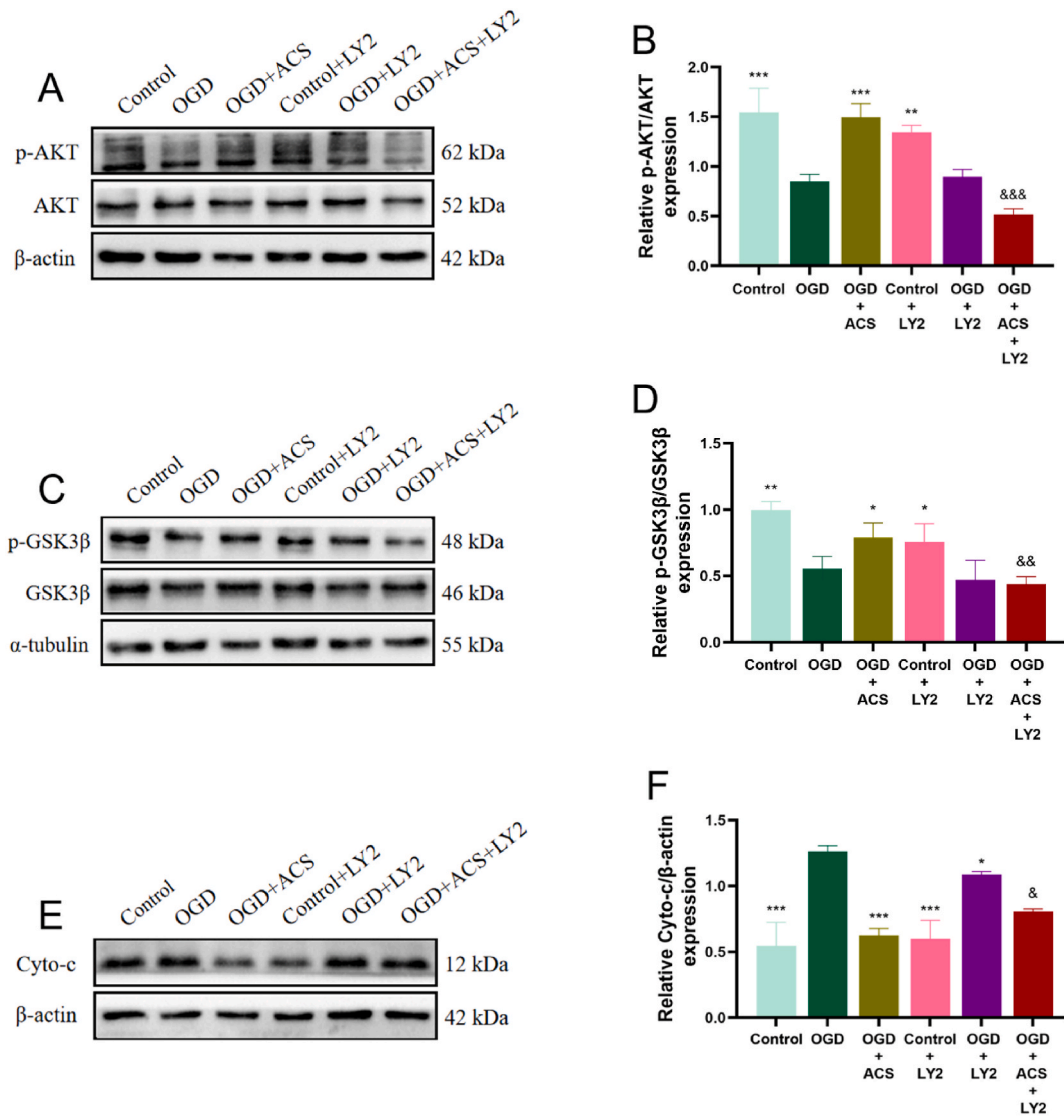
Fig. 11. Effects of the ACS and LY294002 on the protein expression of *p*-AKT/AKT, *p*-GSK3β/GSK3β and Cyto-c in PC12 cells. WB analysis of AKT, *p*-AKT (**A, B**), *p*-GSK3β, GSK3β (**C, D**), Cyto-c (**E, F**). Full-length gels before cropping are noted in fig. S3.Data were presented as mean ± SD (n = 3). *p < 0.05, **p < 0.01 and ***p < 0.001 *vs* OGD group; &p < 0.05, &&p < 0.01 and &&&p < 0.001 *vs* OGD + ACS group.

modulates the PI3K/AKT pathway to inhibit neuronal apoptosis and reduce cerebral ischemic injury, in alignment with predictions from network pharmacology.

5. Conclusion

In brief, our study provides important scientific evidence supporting the role of ACS in combating chronic ischemic neurological injury, potentially through the inhibition of apoptosis. Furthermore, we have demonstrated that the neuroprotective effects of ACS may be associated with the activation of the PI3K/AKT pathway (Fig. 13). These findings offer a theoretical basis for the development of component combinations for anti-CCI in TCM, as well as an experimental basis for the development of novel drugs targeting CCI injury.

Funding
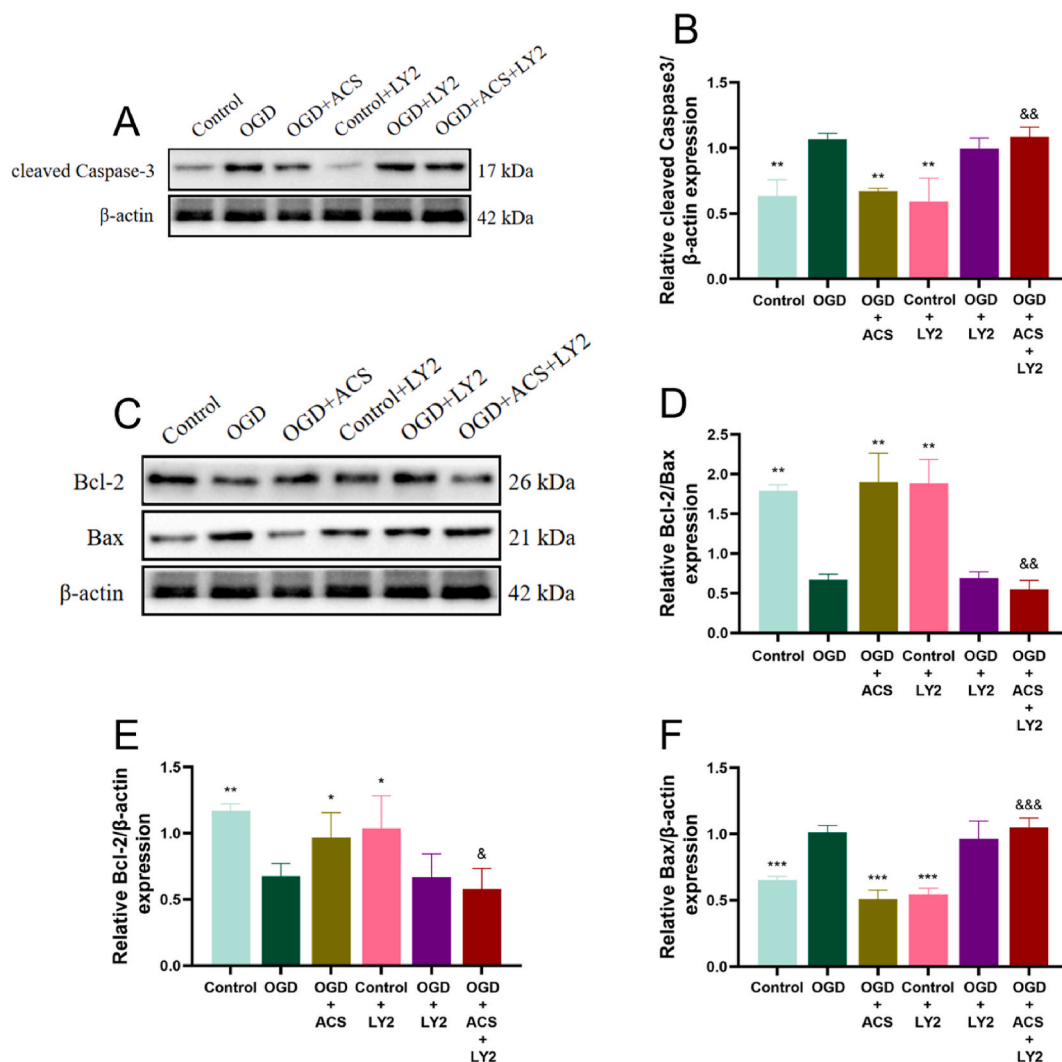
Fig. 12. Effects of the ACS and LY294002 on the protein expression of cleaved Caspase-3, Bcl-2 and Bax in PC12 cells. WB analysis of cleaved-Caspase3 (**A, B**), Bcl-2, Bax, Bcl-2/Bax (**C–F**). Full-length gels before cropping are noted in fig. S4. Data were presented as mean $\pm$ SD (n = 3). $*p < 0.05$, $**p < 0.01$ and $***p < 0.001$ *vs* OGD group; $^\&p < 0.05$, $^{\&\&}p < 0.01$ and $^{\&\&\&}p < 0.001$ *vs* OGD + ACS group.

Data availability statement

Data will be made available on request.

CRediT authorship contribution statement

Declaration of competing interest
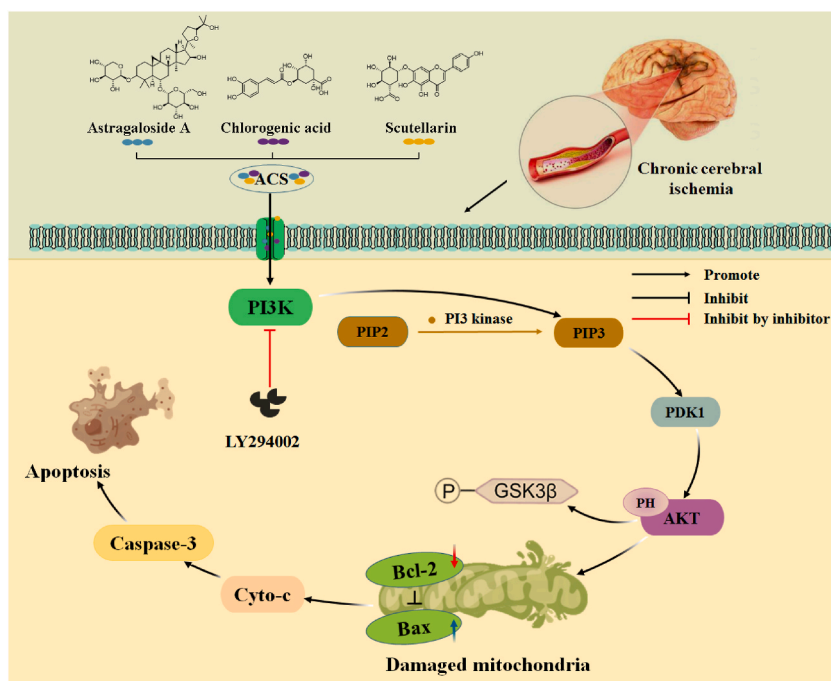
Fig. 13. Mechanism of ACS against CCI injury. CCI induced mitochondrial damage that led to cell apoptosis. ACS exerted neuroprotection by modulating the PI3K/AKT signaling pathway, decreasing the expression of pro-apoptotic factors Bax, Cyto-c, and Caspase-3.

Appendix A. Supplementary data

Supplementary data to this article can be found online at https://doi.org/10.1016/j.heliyon.2024.e29162.

References

[1] M.A. Daulatzai, Cerebral hypoperfusion and glucose hypometabolism: key pathophysiological modulators promote neurodegeneration, cognitive impairment, and Alzheimer's disease, J. Neurosci. Res. 95 (2017) 943–972, https://doi.org/10.1002/jnr.23777.

[2] N. Yan, Z. Xu, C. Qu, J. Zhang, Dimethyl fumarate improves cognitive deficits in chronic cerebral hypoperfusion rats by alleviating inflammation, oxidative stress, and ferroptosis via NRF2/ARE/NF-κB signal pathway, Int. Immunopharm. 98 (2021) 107844, https://doi.org/10.1016/j.intimp.2021.107844.

[3] T. Watanabe, N. Zhang, M. Liu, R. Tanaka, Y. Mizuno, T. Urabe, Cilostazol protects against brain white matter damage and cognitive impairment in a rat model of chronic cerebral hypoperfusion, Stroke 37 (2006) 1539–1545, https://doi.org/10.1161/01.STR.0000221783.08037.a9.

[4] Y. Jia, Z. Li, T. Wang, M. Fan, J. Song, P. Lv, W. Jin, Shikonin Attenuates chronic cerebral hypoperfusion-induced cognitive impairment by inhibiting apoptosis via PTEN/Akt/CREB/BDNF signaling, Evid.-based Compl. Alt. (2021) 2021, https://doi.org/10.1155/2021/5564246.

[5] A. Merelli, M. Repetto, A. Lazarowski, J. Auzmendi, Hypoxia, oxidative stress, and inflammation: three faces of neurodegenerative diseases, J. Alzheimers Dis. 821 (2021) S109–S126, https://doi.org/10.3233/JAD-201074.

[6] L. Poh, D.Y. Fann, P. Wong, H.M. Lim, S.L. Foo, S. Kang, V. Rajeev, S. Selvaraji, V.R. Iyer, N. Parathy, M.B. Khan, D.C. Hess, D. Jo, G.R. Drummond, C.G. Sobey, M.K.P. Lai, C.L. Chen, L.H.K. Lim, T.V. Arumugam, AIM2 inflammasome mediates hallmark neuropathological alterations and cognitive impairment in a mouse model of vascular dementia, Mol. Psychiatr. 26 (2021) 4544–4560, https://doi.org/10.1038/s41380-020-00971-5.

[7] X. Guo, J. Yuan, J. Wang, C. Cui, P. Jiang, Calcitriol alleviates global cerebral ischemia-induced cognitive impairment by reducing apoptosis regulated by VDR/ERK signaling pathway in rat hippocampus, Brain Res. 1724 (2019) 146430, https://doi.org/10.1016/j.brainres.2019.146430.

[8] X. Du, T. Liu, W. Tao, M. Li, X. Li, L. Yan, Effect of aqueous extract of Astragalus membranaceus on behavioral cognition of rats living at high altitude, J. Tradit. Chin. Med. 42 (2022) 58–64, https://doi.org/10.19852/j.cnki.jtcm.2022.01.005.

[9] J. Zhao, Y. Wang, Y. Jin, H. Liu, S. Chen, W. Zhang, H. Peng, Q. Cai, B. Li, H. Yang, H. Zhang, Z. Zhan, Herbal textual research on astragali radix in famous classical formulas, Chin. J. Exp. Tradit. Med. Formulae 28 (2022) 337–346, https://doi.org/10.13422/j.cnki.syfjx.20211659.

[10] N. Wang, H. Sun, X. Ma, Effects of different doses of astragalus injection on neurological rehabilitation of stroke patients, Chin. J. Clin. Ration. Drug Use. 9 (2016) 67–69, https://doi.org/10.15887/j.cnki.13-1389/r.2016.13.039.

[11] T. Guo, Y. Li, Progresses on pharmacological and toxicological effects of Dengzhanxixin injection, China J. Chin. Mater. Med. 37 (2012) 2820–2823, https://doi.org/10.4268/cjcmm20121838.

[12] Y. Yang, Y. Tao, L. Luo, Y. Zhang, X. Wang, X. Meng, Dengzhan Xixin injection derived from a traditional Chinese herb Erigeron breviscapus ameliorates cerebral ischemia/reperfusion injury in rats via modulation of mitophagy and mitochondrial apoptosis, J. Ethnopharmacol. 288 (2022), https://doi.org/10.1016/j.jep.2022.114988.

[13] Y. Lin, Z. Lu, X. Liang, K. Li, B. Peng, J. Gong, Effect of breviscapine against hepatic ischemia reperfusion injury, J. Surg. Res. 203 (2016) 268–274, https://doi.org/10.1016/j.jss.2016.02.013.

[14] H. Tan, T. Yin, Y. Deng, L. He, F. Li, Y. Wang, Mechanisms of Yiqihuoxue herb Naoluoxintong promotes cerebral vascular regeneration in rats with cerebral ischemia syndrome of Qi deficiency accompanied by blood stasis, Chin. J. Cell Mol. Imm. 36 (2020) 712–718, https://doi.org/10.13423/j.cnki.cjcmi.009050.

[15] R. Wu, Y. Liang, M. Xu, K. Fu, Y. Zhang, L. Wu, Z. Wang, Advances in chemical constituents, clinical applications, pharmacology, pharmacokinetics and toxicology of Erigeron breviscapus, Front. Pharmacol. 2 (2021), https://doi.org/10.3389/fphar.2021.656335.

[16] N. Bei, Z. Bei, Y. Wang, D. Long, Y. Wu, X. Fu, P. Liang, L. Li, Clinical study of Dengzhan Xixin injection combined with Astragalus injection in the treatment of acute ischemic stroke, J. Basic Chin. Med. 21 (2015) 1123–1124+1127, https://doi.org/10.19945/j.cnki.issn.1006-3250.2015.09.029.

[17] J. Li, S. Tang, Y. Wu, J. Zeng, J. Zhao, Y. Sheng, Protective effect and mechanism of Astragalus combined with Erigeron breviscapus in the best proportion on cerebral ischemia rats, Pharmacol. Clin. of Chin. Mater. Med. 35 (2019) 104–108, https://doi.org/10.13412/j.cnki.zyyl.2019.02.023.

[18] F. Tian, J. Li, S. Tang, Y. Sun, S. Lin, F. Zhang, X. Xie, Y. Sheng, Optimization of the best proportion of Astragalus membranaceus injection combined with Erigeron breviscapus injection against cerebral ischemia-reperfusion injury in ratsby baseline geometric proportionincreasing and decreasing design, China Pharm. 30 (2019) 1885–1889.

[19] Y. Yan, J. Mi, Y. Fu, F. Cheng, J. Zhang, J. Zeng, Y. Sheng, Effect of combined components of Huangqi and Dengzhanxixin on the oxidative damage in PC12 cells induced by oxygen-glucose deprivation through Nrf2/HO-1 signaling pathway, Pharmacol. Clin. of Chin. Mater. Med. 38 (2022) 159–164, https://doi.org/10.13412/j.cnki.zyyl.20220317.001.

[20] J. Zhang, Y. Yan, F. Cheng, F. Huang, X. Xie, Y. Sheng, Exploring the two herb combination strategy to treat injured PC12 cells, Jove-J. Vis. Exp. (2022), https://doi.org/10.3791/64721.

[21] H. Zhao, Y. Shan, Z. Ma, M. Yu, B. Gong, A network pharmacology approach to explore active compounds and pharmacological mechanisms of epimedium for treatment of premature ovarian insufficiency, Drug Des. Devel. Ther. 13 (2019) 2997–3007, https://doi.org/10.2147/DDDT.S207823.

[22] S. Zhang, Y. Lu, W. Chen, W. Shi, Q. Zhao, J. Zhao, L. Li, Network pharmacology and experimental evidence: PI3K/AKT signaling pathway is involved in the antidepressive roles of chaihu shugan san, Drug Des. Devel. Ther. 15 (2021) 3425–3441, https://doi.org/10.2147/DDDT.S315060.

[23] Q. Cui, Y.L. Zhang, Y.H. Ma, H.Y. Yu, X.Z. Zhao, L.H. Zhang, S.Q. Ge, G.W. Zhang, X.D. Qin, A network pharmacology approach to investigate the mechanism of Shuxuening injection in the treatment of ischemic stroke, J. Ethnopharmacol. 257 (2020) 112891, https://doi.org/10.1016/j.jep.2020.112891.

[24] X. Zhao, J. Liu, L. Yang, Y. Niu, R. Ren, C. Su, Y. Wang, J. Chen, X. Ma, Beneficial effects of mijianchangpu decoction on ischemic stroke through components accessing to the brain based on network pharmacology, J. Ethnopharmacol. 285 (2022) 114882, https://doi.org/10.1016/j.jep.2021.114882.

[25] L. Zhang, L. Han, X. Wang, Y. Wei, J. Zheng, L. Zhao, X. Tong, Exploring the mechanisms underlying the therapeutic effect of Salvia miltiorrhiza in diabetic nephropathy using network pharmacology and molecular docking, Biosci. Rep. 41 (2021), https://doi.org/10.1042/BSR20203520.

[26] F. Wang, L. Wang, F. Liu, L. Meng, N. Zhao, X. Zhai, H. Liu, J. Yang, Investigation of the mechanism of the reduction of anthracycline-induced cardiotoxicity by Qishen Huanwu Capsule based on network pharmacology, Ann. Palliat. Med. 10 (2021) 16–28, https://doi.org/10.21037/apm-20-2204.

[27] D. Szklarczyk, A. Franceschini, S. Wyder, K. Forslund, D. Heller, J. Huerta-Cepas, M. Simonovic, A. Roth, A. Santos, K.P. Tsafou, M. Kuhn, P. Bork, L.J. Jensen, C. von Mering, STRING v10: protein-protein interaction networks, integrated over the tree of life, Nucleic Acids Res. 43 (2015) D447–D452, https://doi.org/10.1093/nar/gku1003.

[28] D. Tian, Q. Gao, Z. Chang, J. Lin, D. Ma, Z. Han, Network pharmacology and *in vitro* studies reveal the pharmacological effects and molecular mechanisms of Shenzhi Jiannao prescription against vascular dementia, BMC Complement. Med. Ther. 22 (2022) 33, https://doi.org/10.1186/s12906-021-03465-1.

[29] J. Wang, L. Peng, L. Jin, H. Fu, Q. Shou, Network pharmacology analysis of the identification of phytochemicals and therapeutic mechanisms of paeoniae radix alba for the treatment of asthma, J. Immunol. Res. 2021 (2021) 9659304, https://doi.org/10.1155/2021/9659304.

[30] Y. Zhou, J. Zhang, L. Wang, Y. Chen, Y. Wan, Y. He, L. Jiang, J. Ma, R. Liao, X. Zhang, L. Shi, Z. Qin, Y. Zhou, Z. Chen, W. Hu, Interleukin-1β impedes oligodendrocyte progenitor cell recruitment and white matter repair following chronic cerebral hypoperfusion, Brain Behav. Immun. 60 (2017) 93–105, https://doi.org/10.1016/j.bbi.2016.09.024.

[31] X. Chai, X. Li, W. Zhang, X. Tan, H. Wang, Z. Yang, Legumain knockout improved cognitive impairment via reducing neuroinflammation in right unilateral common carotid artery occlusion mice, Life Sci. 285 (2021) 119944, https://doi.org/10.1016/j.lfs.2021.119944.

[32] Y. Li, H. Ding, X. Fu, S. Tang, Z. Lu, F. Yang, X. Liu, C. Deng, Effect of astragaloside IV combined with Panax notoginseng saponins on nerve repair after BMSCs transplantation in rats with cerebral ischemia, Chin. Tradit. Herb. Drugs 52 (2021) 6537–6544.

[33] A.R. Wang, L.F. Mi, Z.L. Zhang, M.Z. Hu, Z.Y. Zhao, B. Liu, Y.B. Li, S. Zheng, Saikosaponin A improved depression-like behavior and inhibited hippocampal neuronal apoptosis after cerebral ischemia through p-CREB/BDNF pathway, Behav. Brain Res. 403 (2021) 113138, https://doi.org/10.1016/j.bbr.2021.113138.

[34] J. Zhang, Y. Yan, F. Cheng, F. Huang, X. Xie, Y. Sheng, Exploring the two herb combination strategy to treat injured PC12 cells, J. Vis. Exp. (2022), https://doi.org/10.3791/64721.

[35] Y. Wang, Z. Li, H. Gu, Y. Zhai, Y. Jiang, X. Zhao, Y. Wang, X. Yang, C. Wang, X. Meng, H. Li, L. Liu, J. Jing, J. Wu, A. Xu, Q. Dong, D. Wang, J. Zhao, China stroke statistics 2019: a report from the national center for healthcare quality management in neurological diseases, China national clinical research center for neurological diseases, the Chinese stroke association, national center for chronic and non-communicable disease control and prevention, Chinese center for disease control and prevention and institute for global neuroscience and stroke collaborations, stroke vasc, Neurol. 5 (2020) 211–239, https://doi.org/10.1136/svn-2020-000457.

[36] Y. Ye, X. Yan, J. Li, G. Mei, Y. Luo, S. Zhong, Effect of Astragalus membranaceus and Dengzhanxixin injection on serum NSE levels in patients with acute cerebral infarction, J. Emerg. Tradit. Chin. Med. (2005) 1177–1178+1225.

[37] S. Li, B. Zhang, Traditional Chinese medicine network pharmacology: theory, methodology and application, Chin. J. Nat. Med. 11 (2013) 110–120, https://doi.org/10.1016/S1875-5364(13)60037-0.

[38] S. Li, Exploring traditional Chinese medicine by a novel therapeutic concept of network target, Chin. J. Integr. Med. 22 (2016) 647–652, https://doi.org/10.1007/s11655-016-2499-9.

[39] Q. Zeng, Z. Huang, J. Zhang, R. Liu, X. Li, J. Zeng, H. Xiao, 3'-Daidzein sulfonate sodium protects against chronic cerebral hypoperfusion-mediated cognitive impairment and hippocampal damage via activity-regulated cytoskeleton-associated protein upregulation, Front. Neurosci. 13 (2019) 104, https://doi.org/10.3389/fnins.2019.00104.

[40] M. Ihara, Y. Yamamoto, Emerging evidence for pathogenesis of sporadic cerebral small vessel disease, Stroke 47 (2016) 554–560, https://doi.org/10.1161/STROKEAHA.115.009627.

[41] J. Duncombe, A. Kitamura, Y. Hase, M. Ihara, R.N. Kalaria, K. Horsburgh, Chronic cerebral hypoperfusion: a key mechanism leading to vascular cognitive impairment and dementia. Closing the translational gap between rodent models and human vascular cognitive impairment and dementia, Clin. Sci. (Lond) 131 (2017) 2451–2468, https://doi.org/10.1042/CS20160727.

[42] K. Yoshizaki, K. Adachi, S. Kataoka, A. Watanabe, T. Tabira, K. Takahashi, H. Wakita, Chronic cerebral hypoperfusion induced by right unilateral common carotid artery occlusion causes delayed white matter lesions and cognitive impairment in adult mice, Exp. Neurol. 210 (2008) 585–591, https://doi.org/10.1016/j.expneurol.2007.12.005.

[43] L. Xiang, Y. Li, L. Cao, M. Miao, Animal model analysis on chronic cerebral hypoperfusion based on clinical symptom characteristics, Tradit. Chin. Drug Res. Clin. Pharmacol. 32 (2021) 93–98, https://doi.org/10.19378/j.issn.1003-9783.2021.01.013.

[44] D. Chen, C. Peng, X. Xie, Q. Chen, H. Liu, S. Zhang, F. Wan, H. Ao, Low dose of anisodine hydrobromide induced neuroprotective effects in chronic cerebral hypoperfusion rats, CNS Neurol. Disord.: Drug Targets 16 (2017) 1111–1119, https://doi.org/10.2174/1871527316666171026114043.

[45] Y. Sun, Z. Zhao, Q. Li, C. Wang, X. Ge, X. Wang, G. Wang, Y. Qin, Dl-3-n-butylphthalide regulates cholinergic dysfunction in chronic cerebral hypoperfusion rats, J. Int. Med. Res. 48 (2020) 300060520936177, https://doi.org/10.1177/0300060520936177.

[46] E. Arslan, M.O. Biyik, M. Kosucu, A.R. Guvercin, A. Bodur, A. Alver, Is ceftriaxone effective in experimental brain ischemia/reperfusion injury? Bratisl. Lek. Listy 121 (2020) 858–863, https://doi.org/10.4149/BLL_2020_141.

[47] J.L. Yang, S. Mukda, S.D. Chen, Diverse roles of mitochondria in ischemic stroke, Redox Biol. 16 (2018) 263–275, https://doi.org/10.1016/j.redox.2018.03.002.

[48] S.S. Andrabi, S. Parvez, H. Tabassum, Ischemic stroke and mitochondria: mechanisms and targets, Protoplasma 257 (2020) 335–343, https://doi.org/10.1007/s00709-019-01439-2.

[49] K.S. Panickar, R.A. Anderson, Effect of polyphenols on oxidative stress and mitochondrial dysfunction in neuronal death and brain edema in cerebral ischemia, Int. J. Mol. Sci. 12 (2011) 8181–8207, https://doi.org/10.3390/ijms12118181.

[50] T.H. Sanderson, C.A. Reynolds, R. Kumar, K. Przyklenk, M. Hüttemann, Molecular mechanisms of ischemia-reperfusion injury in brain: pivotal role of the mitochondrial membrane potential in reactive oxygen species generation, Mol. Neurobiol. 47 (2013) 9–23, https://doi.org/10.1007/s12035-012-8344-z.

[51] M.S. Sun, H. Jin, X. Sun, S. Huang, F.L. Zhang, Z.N. Guo, Y. Yang, Free radical damage in ischemia-reperfusion injury: an obstacle in acute ischemic stroke after revascularization therapy, Oxid. Med. Cell. Longev. 2018 (2018) 3804979, https://doi.org/10.1155/2018/3804979.

[52] Z.Q. Yan, J. Chen, G.X. Xing, J.G. Huang, X.H. Hou, Y. Zhang, Salidroside prevents cognitive impairment induced by chronic cerebral hypoperfusion in rats, J. Int. Med. Res. 43 (2015) 402–411, https://doi.org/10.1177/0300060514566648.

[53] Z. Zhang, L. Yao, J. Yang, Z. Wang, G. Du, PI3K/Akt and HIF-1 signaling pathway in hypoxia-ischemia, Mol. Med. Rep. 18 (2018) 3547–3554, https://doi.org/10.3892/mmr.2018.9375 (Review).

[54] F. Yin, H. Zhou, Y. Fang, C. Li, Y. He, L. Yu, H. Wan, J. Yang, Astragaloside IV alleviates ischemia reperfusion-induced apoptosis by inhibiting the activation of key factors in death receptor pathway and mitochondrial pathway, J. Ethnopharmacol. 248 (2020) 112319, https://doi.org/10.1016/j.jep.2019.112319.

[55] M. Zhu, M. Liu, Q.L. Guo, C.Q. Zhu, J.C. Guo, Prolonged DADLE exposure epigenetically promotes Bcl-2 expression and elicits neuroprotection in primary rat cortical neurons via the PI3K/Akt/NF-κB pathway, Acta Pharmacol. Sin. 39 (2018) 1582–1589, https://doi.org/10.1038/aps.2018.7.

[56] J. Meng, H. Ma, Y. Zhu, Q. Zhao, Dehydrocostuslactone attenuated oxygen and glucose deprivation/reperfusion-induced PC12 cell injury through inhibition of apoptosis and autophagy by activating the PI3K/AKT/mTOR pathway, Eur. J. Pharmacol. 911 (2021) 174554, https://doi.org/10.1016/j.ejphar.2021.174554.